AGU PUBLICATIONS

Water Resources Research

RESEARCH ARTICLE
10.1002/2015WR018150

Key Points:
- A 3-D numerical model for root water uptake that considers rhizosphere properties is developed
- Numerical results are in a qualitative agreement with recent experiments
- Rhizosphere properties tend to buffer bulk soil water content variation under transient irrigation

Correspondence to:
N. Schwartz,
nimrod.schwartz@uclouvain.be

Citation:
Schwartz, N., A. Carminati, and M. Javaux (2016), The impact of mucilage on root water uptake—A numerical study, *Water Resour. Res.*, *52*, 264–277, doi:10.1002/2015WR018150.

Received 24 SEP 2015
Accepted 22 DEC 2015
Accepted article online 22 DEC 2015
Published online 14 JAN 2016

The impact of mucilage on root water uptake—A numerical study

N. Schwartz[1], A. Carminati[2], and M. Javaux[1,3]

[1]Earth and Life Institute/Environmental Sciences, Université catholique de Louvain, Louvain-la-Neuve, Belgium, [2]Division of Soil Hydrology, Georg August University of Goettingen, Goettingen, Germany, [3]Agrosphere, IBG-3 Forschungszentrum, Juelich GmbH, Juelich, Germany

Abstract The flow of water between soil and plants follows the gradient in water potential and depends on the hydraulic properties of the soil and the root. In models for root water uptake (RWU), it is usually assumed that the hydraulic properties near the plant root (i.e., in the rhizosphere) and in the bulk soil are identical. Yet a growing body of evidence has shown that the hydraulic properties of the rhizosphere are affected by root exudates (specifically, mucilage) and markedly differ from those of the bulk soil. In this work, we couple a 3-D detailed description of RWU with a model that accounts for the rhizosphere-specific properties (i.e., rhizosphere hydraulic properties and a nonequilibrium relation between water content and matric head). We show that as the soil dries out (due to water uptake), the higher water holding capacity of the rhizosphere results in a delay of the stress onset. During rewetting, nonequilibrium results in a slower increase of the rhizosphere water content. Furthermore, the inverse relation between water content and relaxation time implies that the drier is the rhizosphere the longer it takes to rewet. Another outcome of nonequilibrium is the small fluctuation of the rhizosphere water content compared to the bulk soil. Overall, our numerical results are in agreement with recent experimental data and provide a tool to further examine the impact of various rhizosphere processes on RWU and water dynamics.

1. Introduction

Root water uptake (RWU) is a key component of the hydrological cycle, accounting for 80–90% of the total terrestrial evapotranspiration [e.g., *Jasechko et al.*, 2013]. Essentially, all the water used by plants is extracted from the soil by the roots. Water fluxes in the soil-plant system follow water potential gradients along flow path and are largely controlled by the hydraulic properties of the soil and the root system [*Tuzet et al.*, 2003; e.g., *Garrigues et al.*, 2006]. The water flow around a root segment between the bulk soil and the soil-root interface can be represented by the radial Richards equation [e.g., *Gardner*, 1960; *de Jong van Lier et al.*, 2007; *Schroeder et al.*, 2008]. In the root system, when water capacity is neglected, water potential and flux distributions between soil-root interface and root collar can be modeled with simple equations similar to Ohm's law [*Landsberg and Fowkes*, 1978; *Doussan*, 1998]. Root-soil interface water potential distribution is thus crucial to estimate water uptake distribution and soil water redistribution. Recently, numerical models, which couple soil and root system equation to resolve the 3-D distribution of water flow in the soil-plant system, have been proposed [*Garrigues et al.*, 2006; *Javaux et al.*, 2008; *Schneider et al.*, 2009].

Typically, soil-root interface and the bulk soil properties are considered as being the same in root water uptake simulations. Yet for many years, it has been known that the soil in close vicinity of the root (i.e., the rhizosphere) has unique biological, chemical, and physical properties (the term rhizosphere was coined by Lorenz Hiltner in 1904 [see *Hartmann et al.*, 2007]). While the biological and chemical properties of the rhizosphere have been studied for many years [e.g., *Rovira*, 1956], the physical properties of the rhizosphere and their impact on water flow and RWU are just now beginning to receive more attention [e.g., *Carminati and Vetterlein*, 2013].

Recently, neutron tomography studies demonstrated that during period of drying the water content in the rhizosphere is greater than in the bulk soil [*Carminati et al.*, 2010; *Moradi et al.*, 2011]. This is a nonintuitive finding as if there was no difference between the hydraulic properties of the bulk soil and the rhizosphere, we would expect a decrease in water content with a decreasing distance to the root surface. In addition, after

wetting dry soil, *Moradi et al*. [2011] showed that while the water content in the bulk soil rapidly increases, the rhizosphere remains drier. In this case, only after approximately 24 h from rewetting, the water content in the bulk soil and in the rhizosphere seems to equalized (similar drying-wetting dynamics were also reported by *Carminati* [2013], *Carminati and Vetterlein* [2013], and *Moradi et al*. [2012]). To explain this nontrivial water dynamics behavior in the rhizosphere, *Carminati and Vetterlein* [2013] suggested that mucilage released by the root alters the hydraulic properties of the rhizosphere, hence explaining the observed drying-wetting dynamics. The most relevant mucilage properties are its high water holding capacity [*Ahmed et al*., 2014; *Ghezzehei and Albalasmeh*, 2015; *McCully and Boyer*, 1997] , its relatively low surface tension [*Read and Gregory*, 1997], and the relatively high viscosity of mucilage [*Kroener et al*., 2014; *Zarebanadkouki and Carminati*, 2014]. *Aravena et al*. [2013] suggested that compaction of the rhizosphere by the root can also explain the increase in the rhizosphere water holding capacity [see also *Daly et al*., 2015].

Carminati [2012] recently developed a model that couples rhizosphere processes and RWU. In this 1-D model, two regions are defined: the bulk soil and the rhizosphere. Each of these regions is characterized by a set of homogeneous hydraulic functions (retention curve and hydraulic conductivity) and for the rhizosphere nonequilibrium between water content and matric head is also considered. Using a steady-rate approximation (i.e., $\partial\theta/\partial t$=const.), an analytic solution of the model was proposed. The model was able to reproduce the observed water dynamics in the rhizosphere. *Kroener et al*. [2014] used the conceptual model of *Carminati* [2012] and developed a numerical solution for the soil-rhizosphere flow problem (in this model RWU was not considered). *Kroener et al*. [2014] assumed a gradual transition in the rhizosphere properties (as a function of distance from the root). This model was tested against an experiment in which the water dynamics of soil mixed with mucilage was measured. The agreement between the model and the experiment reported by *Kroener et al*. [2014] supports the model assumptions with regard to the impact of mucilage on rhizosphere properties and hence on water dynamics (a detail description of the model is given in section 2).

The specific hydraulic properties of the rhizosphere may have an impact on RWU distribution and dynamics. For instance, it could be expected that the high water adsorption capacity of mucilage affects the rhizosphere water retention curve by increasing the water content of the rhizosphere for a given matric head. In turn, the increased water content would result in a higher hydraulic conductivity of the rhizosphere. A change in rhizosphere hydraulic conductivity may alter the soil-root interface potential for a given local uptake. At the root system scale, the distribution of the rhizosphere properties will change the spatial distribution of hydraulic conductivity and potential at the soil-root interface and also RWU spatial distribution. If, in addition, rhizosphere dynamics differs from bulk soil, it could also be expected that the stress onset will be impacted. Modeling the soil-rhizosphere-plant system with a mechanistic approach may thus help to decipher the impact of rhizosphere properties on magnitude and distribution of uptake.

The objective of this work is to assess how small-scale processes in the rhizosphere affect plant scale response such as stress onset, RWU distribution, and water dynamics in the soil. To achieve this goal, we coupled, for the first time, a detailed 3-D RWU model and a model that considers rhizosphere hydraulic properties (retention and conductivity functions) and nonequilibrium between water content and matric head.

2. Model Description

In this section, we briefly describe the main equations used to couple the rhizosphere and the soil-plant model.

2.1. Main Flow Equations

To account for the impact of rhizosphere properties on RWU, we coupled a 3-D model for water flow in soil and root (R-SWMS) [see *Javaux et al*., 2008] with the rhizosphere model developed by *Kroener et al*. [2014]. We start with the classical 3-D Richards equation [*Richards*, 1931] for soil water flow

$$\frac{\partial\theta_T}{\partial t}=\nabla\cdot[K\nabla(h-z)]-S \tag{1}$$

where θ_T $(\mathrm{cm^3 cm^{-3}})$ is the total volumetric water content in the soil, K $(\mathrm{cm\,d^{-1}})$ is the hydraulic conductivity, h (cm) is the matric head, z (cm) is the gravitational head (positive downward), and S $(\mathrm{cm^3\,cm^{-3}\,d^{-1}})$ is

the water sink term (positive for uptake). The total water content in a soil element is the sum of the relative contribution of water content in pores with and without mucilage:

$$\theta_T = R\theta_b + (1-R)\theta_m \tag{2}$$

where $R = 1 - V_m/V_p$ is a weighting factor that accounts for the volume fraction of pores not occupied by mucilage, and it tends to 1 far away from roots. V_m is the volume of pores invaded by mucilage, and V_p is the total pore volume. The water content in the fraction of pores with and without mucilage is θ_m and θ_b, respectively.

Nonequilibrium dynamics in the rhizosphere is introduced with a kinetic equation [*Hassanizadeh et al.*, 2002; *Kroener et al.*, 2014]

$$\frac{\partial \theta_m}{\partial t} = \frac{1}{\tau(\theta_m)}(h - h_{eq}) \tag{3}$$

where $\tau\,(\mathrm{cm\,d})$ is the relaxation time and $h_{eq}\,(\mathrm{cm})$ is the "equilibrium pressure head," to which the actual matric head converge for a long equilibration time with no change of boundary conditions. Nonequilibrium arises from the noninstantaneous swelling/shrinking of the gel network, during imbibition/drainage [*Kroener et al.*, 2014]. Note that according to equation (3), the system reaches equilibrium when $h = h_{eq}$ and that the rate of this process depends on the relaxation time (large relaxation time means slow change in water content and hence long time to reach equilibrium).

Taking the time derivative of equation (2) and using equations (1) and (3), we get the main flow equation in the soil

$$\frac{\partial \theta_T}{\partial t} = R\frac{\partial \theta_b}{\partial t} + (1-R)\frac{1}{\tau}(h - h_{eq}) = \nabla \cdot [K\nabla(h - z)] - S \tag{4}$$

Using the definition for specific soil water holding capacity $(C_b = \partial\theta_b/\partial h)$, we can write equation (4) in terms of matric head

$$RC_b\frac{\partial h}{\partial t} + (1-R)\frac{1}{\tau}(h - h_{eq}) = \nabla \cdot [K\nabla(h - z)] - S \tag{5}$$

Note that when $R = 1$ (i.e., the volume of mucilage is zero), the second term on the left-hand side of equation (5) is canceled and we have the classical Richards equation.

2.2. Hydraulic Properties

The water retention curve for both the bulk soil and rhizosphere is modeled based on Brooks & Corey function [*Brooks and Corey*, 1964].

$$\Theta = \begin{cases} (h_{cr}/h)^{\lambda} & ; \quad h < h_{cr} \\ 1 & ; \quad h \geq h_{cr} \end{cases} \tag{6}$$

where $\Theta = (\theta - \theta_r)/(\theta_s - \theta_r)$ is the water saturation degree, θ_s and θ_r are the saturated and residual water content, respectively, $h_{cr}\,(\mathrm{cm})$ is the critical matric head (also known as the air entry value), and λ is a fitting parameter. As suggested by *Kroener et al.* [2014], the relationship between rhizosphere water content and the equilibrium pressure head (h_{eq}) is given by

$$h_{eq} = h(\theta_T) - \omega_o\left(\frac{c_w}{\theta_m}\right)^{\beta} \tag{7}$$

where $\omega_0\,(\mathrm{cm})$ and β are fitting parameters and $c_w = (c_{tot}\rho_b)/(\theta_m\rho_w)$ is the concentration of mucilage in water, $c_{tot}\,(\mathrm{g\,g^{-1}})$ is the ratio between dry weight of mucilage to dry weight of soil, ρ_b and ρ_w (unit of $\mathrm{g\,cm^{-3}}$) are the bulk soil and water density, respectively. The equilibrium retention curve (equation (7)) means that at a given soil water content, the presence of mucilage decreases the soil matric potential. Furthermore, higher concentration of mucilage results in a higher water retention curve (for more details, see *Kroener et al.* [2014]).

A modified hydraulic conductivity function, which is based on the Mualem-Brooks-Corey model [*Brooks and Corey*, 1964; *Mualem*, 1976] and that consider mucilage viscosity is given by [*Ahmed et al*., 2014]

$$K=\frac{1}{\mu(c_w)}K_b \tag{8}$$

where $\mu=1+\nu c_w^d$ is the relative viscosity of mucilage (compared to water), ν and d are unitless fitting parameters and $K_b=K_s\Theta_T^{2/\lambda+2+L}$ is the unsaturated hydraulic conductivity function where $K_s\,(\mathrm{cm\,d^{-1}})$ is the saturated hydraulic conductivity and L is a fitting parameter. Note that wherever mucilage concentration is zero, equation (8) reduces to its classical form.

Lastly, the relaxation time, which accounts for the rate of the system to reach equilibrium is related to the water content. The reason is that with decreasing water content the average distance between the polymers decreases too. A power law relation between water content and relaxation time was found to well represent the experimental results [*Kroener et al*., 2014]

$$\tau=\theta_m^{-\gamma}\tau_0 \tag{9}$$

where γ and $\tau_0\,(\mathrm{cm\,d})$ are fitting parameters.

The sink term S in equation (5) is calculated by explicitly solving the radial and axial flows in the 3-D root system [*Javaux et al*., 2008]. For one root segment of length l, the radial flow $J_r\,(\mathrm{cm^3\,d^{-1}})$ between the soil and the root is given by

$$J_r=k_rA_r(h-h_x) \tag{10}$$

where $k_r\,(\mathrm{d^{-1}})$ is the intrinsic radial conductivity of the root, $A_r\,(\mathrm{cm^2})$ is the outer surface area of a root segment, and $h_x\,(\mathrm{cm})$ is the xylem pressure head. The axial flow $J_x\,(\mathrm{cm^3\,d^{-1}})$ (i.e., flow in the xylem) is

$$J_x=-k_x\left(\frac{\Delta h_x}{l}+\frac{\Delta z}{l}\right) \tag{11}$$

where $k_x\,(\mathrm{cm^3\,d^{-1}})$ is the xylem conductivity. The system of equations is closed by applying boundary condition at the root collar (the upper most part of the xylem). The Sink can then be calculated by integrating the radial fluxes per soil voxel j with

$$S_j=\frac{\sum_i^n J_{r,i}}{V_j} \tag{12}$$

where $V_j\,(\mathrm{cm^3})$ is the volume of the soil voxel and n is the number of root segments within voxel j.

3. Material and Methods

3.1. Scenario Descriptions

To account for the impact of mucilage on RWU and to isolate the effects of rhizosphere hydraulic properties and nonequilibrium on water flow and root water uptake, three different scenarios were considered. The first scenario, "Control," solves the classical Richards equation where both the rhizosphere and the bulk soil properties are identical and no kinetic equation is considered. The soil hydraulic properties (sandy soil) for this scenario were obtained from *Kroener et al.* [2014] and are reported in Table 1. In the second scenario, "Static," the hydraulic properties of the rhizosphere differ from those of the bulk soil, but an equilibrium between the water potential and the water content is assumed (no kinetic equation). In other words, in this scenario, we solve equation (1) but we define two regions, the rhizosphere and the bulk soil each with a different hydraulic properties (retention and conductivity functions). We obtained the Brooks and Corey parameters set for the "Static" scenario by solving equation (7) for h_{eq} and fitting the $h_{eq}(\theta)$ relationship to equation (6). The resultant Brooks and Corey parameters for the "Static" scenario are $\lambda_r=0.33$ and $h_{cr,r}=-25.9$ cm. In addition, in this scenario, the impact of mucilage on the hydraulic conductivity function of the rhizosphere was also considered (see equation (8)). In Table 2, the relevant parameters set for the "Static" scenario are given. Note that the bulk hydraulic properties of this scenario are identical to the "Control" scenario (i.e., for the bulk soil, the parameters are given in Table 1 and for the rhizosphere in Table 2).

Table 1. Hydraulic Properties of the Soil (Bulk + Rhizosphere) for the "Control" Scenario[a]

θ_s	θ_r	λ	h_{cr} (cm)	K_s (cm d^{-1})	L
0.41	0.02	0.7	−13.6	732	2

[a]Note that those properties were also used as the bulk soil properties for all the scenarios used in this study.

In the "Dynamic" scenario, the full coupled model presented in section 2 is considered. The hydraulic properties of the rhizosphere for this scenario are identical to the "Static" scenario and are given in Table 2. The bulk soil properties for the "Dynamic" scenario are identical to the "Control" and "Static" scenarios (Table 1). The difference between the "Dynamic" and "Static" scenarios is that in the former nonequilibrium is also considered. As mentioned before, nonequilibrium results in a nonunique relation between the water content and the matric head. Therefore, despite the fact that the hydraulic parameters of the "Static" and "Dynamic" scenarios are identical, the retention and hydraulic conductivity functions of the "Dynamic" scenario also depend on the relaxation time and on the history of the water content. Note that since the rhizosphere in this work is defined to occupy one soil voxel around the root, for both the "Dynamic" and "Static" scenarios, the weighting factor that accounts for the volume fraction of pores occupied by mucilage (R) is constant. The value of R (see Table 2) was chosen with accordance to *Ahmed et al.* [2014].

3.2. Domain Geometry, Boundary, and Initial Conditions

As our first objective was to investigate interactions between rhizosphere and water uptake processes, a simple scenario was set up with a single root into a small container and a fine spatial resolution in order to accurately simulate soil water potential gradients. The model domain is a $3\times3\times8$ cm^3 box. The domain is discretized into 7.2×10^4 cubical elements of $0.1\times0.1\times0.1$cm^3 each. A single root of 5 cm long and 1 mm in diameter is located in the middle of the domain. A simple young root with a constant intrinsic radial conductivity of 1.9×10^{-4} day^{-1} and axial conductance of 4.32×10^{-2} cm^3 d^{-1} was chosen [*Doussan*, 1998]. An isohydric root boundary condition is defined at the root collar according to:

$$\mathrm{BC}_{collar}=\begin{cases} T_p(t) & ; \quad H_{collar} > H_{stress} \\ H_{stress} & ; \quad else \end{cases} \tag{13}$$

where T_P (cm^3 d^{-1}) is the potential transpiration, H_{collar} (cm) is the total water head at the root collar, and $H_{stress}=-2\times10^3$ cm is the lowest allowable value of the total collar water head. That is, as $H_{collar}=H_{stress}$, the potential transpiration cannot be met by the soil and the plant experience water stress, i.e., the actual water collar flux is lower than the potential one (T_p).

For each scenario ("Control," "Static," and "Dynamic," see section 3.1), three different setups were examined; drying soil, wetting soil, and drying and wetting cycles. In the drying setup, the soil ($h(t=0)=-150$ cm) is exposed to a constant potential transpiration ($T_p=0.5$ cm^3 d^{-1}). The boundaries of the soil domain were set to zero flux. The wetting setup started at day 10 of the drying (i.e., the initial condition of the wetting was determined by the last time step of the drying). In this setup, a short flux was introduced from the top boundary of the domain ($q_{top}=55.55$ cm d^{-1} for 0.01 day, i.e., ~ 5 cm^3). The amount of water added in this setup is equal to the potential transpiration. In order to investigate the impact of rhizosphere processes on the rewetting of a very dry soil (note that the lowest possible matric head in the drying setup is confined by H_{stress}), we also run a simulation in which an initially dry soil ($h(t=0)=-1\times10^4$ cm) is exposed to a flux of water ($q_{top}=730$ cm d^{-1} for 0.02 day, i.e., ~ 131 cm^3) from the upper boundary of the domain. In this case, the bottom boundary of the domain was set to free drainage. In order to reach saturated conditions, the flux was chosen to be equal to the saturated hydraulic conductivity ($q_{top}=K_s$).

Table 2. Parameter Set for the Hydraulic Properties of the "Static" and "Dynamic" Scenarios[a]

Parameter	Unit	value
ω_0	cm	1.22×10^6
β		3.8
c_T	g g^{-1}	0.0125
ρ_b	g cm^{-3}	1.65
ρ_w	g cm^{-3}	1.0
ν		566
d		1.4
τ_0	cm d	160
γ		4
R		0.286

[a]The parameters were obtained from *Kroener et al.* [2014] and *Ahmed et al.* [2014]. Note that these parameters are only valid for the rhizosphere. For the bulk soil, see Table 1.

In the third setup (drying and wetting cycle), the daily potential transpiration was also set to 0.5 cm^3 d^{-1}. In this setup, the soil was uniformly irrigated from the top ($q_{top}=150$ cm d^{-1} for 0.05 day) every 15 days. In this setup, the amount of

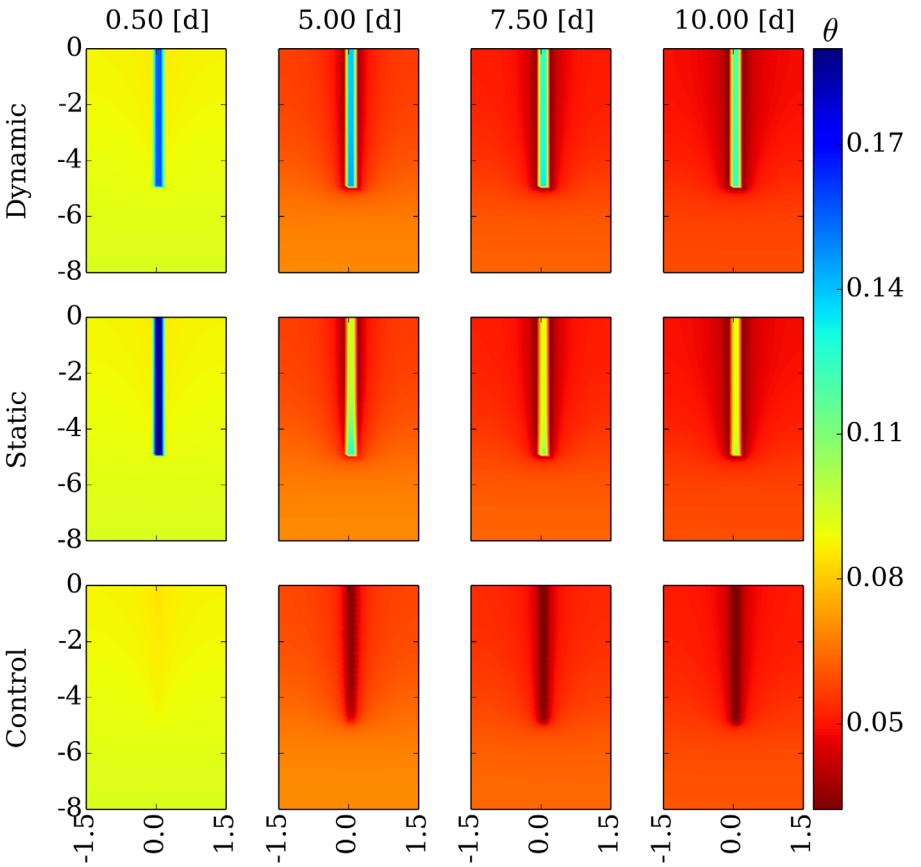

Figure 1. A vertical cross section (y = 0) of the water content distribution for the different scenarios at different times. Note that the *x* and *z* axis represent the width and depth (in cm) of the domain, respectively, and that for better visibility of the root-soil interface, the horizontal and vertical scales are not equal.

water added at each cycle is 9 times higher than the potential transpiration for that period, so the initial condition at the beginning of each cycle did not depend on the final conditions of the previous cycle. In addition, the flux was low enough to keep the soil unsaturated. The two different initial conditions that were used in the wetting setup were also used here (−150 and −15,000 cm). With this scenario, we wanted to investigate whether cumulative effect of the rhizosphere-specific processes could occur.

4. Results

4.1. Drying Soil

In the drying setup, a soil with an initial uniform matric head $(h=-150\ \text{cm})$ is exposed to a constant transpiration demand (see equation (13)) which results in a water depletion in the rhizosphere and in the bulk soil (see Figure 1). Half a day from the beginning of the simulation, two patterns of water content distributions are observed. For the "Control" scenario, a homogeneous soil water distribution develops while for the "Static" and "Dynamic" scenarios, the water content in the rhizosphere (close to the root, around x = 0) is higher than in the bulk soil (far from the root). Those patterns illustrate how the differences between the hydraulic properties of the rhizosphere and the bulk soil affect water content distribution in the soil.

With time, water distribution patterns develop differently between scenarios. As expected, for the "Control" scenario, the rhizosphere becomes dryer than the bulk soil. This is the expected distribution since it is commonly assumed that the bulk and rhizosphere hydraulic properties are identical [*Roose and Fowler*, 2004; *Doussan et al*., 2006; *Javaux et al*., 2008; *Schneider et al*., 2009]. For both the "Static" and "Dynamic" scenarios, the water content in the rhizosphere is higher than in the bulk soil. For example, at $t=10$ days, the bulk and rhizosphere average water content for the "Static" scenario are 0.053 and 0.089, respectively. For the "Dynamic" scenario, the difference between the bulk and rhizosphere water content is higher (average

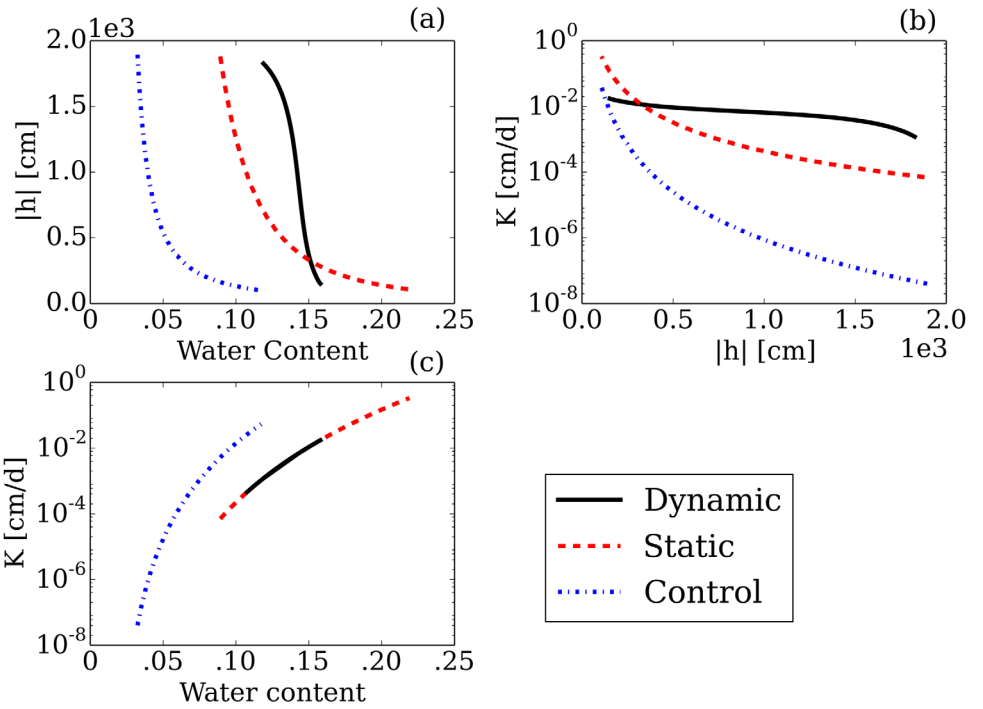

Figure 2. Relation between water content, matric potential, and hydraulic conductivity in a point of the rhizosphere during the drying period for the different scenarios. The retention curve is shown in Figure 2a, the hydraulic conductivity as a function of matric head absolute value and water content are shown in Figures 2b and 2c, respectively. The bulk hydraulic properties of both the "Dynamic" and "Static" scenarios (i.e., far from the root) are identical to the properties on the "Control" scenario. Note that the data were obtained from the model results at one point (0, 0, −2).

water content of 0.052 for the bulk soil and 0.118 for the rhizosphere). Under those conditions, nonequilibrium dynamics between water content and matric head results in a wetter rhizosphere and a drier bulk soil. That is as the rate of change in water content under nonequilibrium condition is lower than under equilibrium condition (see, for example, equation (4)).

The hydraulic properties of the rhizosphere (obtained by plotting the model results at $x=y=0$, $z=-2$) for the different scenarios are shown in Figure 2. For the "Static" and "Control" scenarios, both the retention and the conductivity functions are identical to the curves that would be obtained if we simply plotted equations (6) and (8) (i.e., the hydrostatic curves), while for the "Dynamic" scenario, the retention curve cannot be calculated a priori (this is due to the nonequilibrium between water content and matric head).

In Figure 2b, the evolution of hydraulic conductivity values as a function of the matric head absolute values are shown for the different scenarios. The hydraulic conductivity curves of the "Static" and "Dynamic" scenarios cross each other. For matric heads lower than −300 cm (dryer soil), the hydraulic conductivity of "Dynamic" scenario is higher than the "Static" one. Furthermore, the slope of the "Dynamic" conductivity curve is much smaller than the slopes of the "Static" and "Control" scenarios. This is because the range of water content for the "Dynamic" scenario is the lowest (see Figure 2a). Note that the same relation between conductivity and water content is observed for the "Static" and "Dynamic" scenarios (Figure 2c).

In Figure 3a, the xylem total water head at the root collar (H_{collar}) as a function of time is shown for the different scenarios (recall that the collar is the upper most part of the root). Until 1 day from the beginning of the simulations, H_{collar} is similar for all scenarios. A steep decrease in H_{collar} is first observed for the "Control" scenario and then for the "Static" and the "Dynamic" scenarios. For the "Control" scenario, stress starts (the time where $H_{collar}=-2\times10^3$ cm for the first time) at day 2.75 while for the "Dynamic" and "Static" scenarios, stress onset at day 3.2 (i.e., 10 h after stress onset of the "Control" scenario). The lag in the stress onset for the "Dynamic" and "Static" scenario is due to the bigger rhizosphere hydraulic conductivity in those scenarios (see Figure 2b) and the resultant smaller hydraulic gradient required to sustain transpiration demand. As soon as $H_{collar}=-2\times10^3$ cm, transpiration rate starts to decrease (see Figure 3b). The relative transpiration (ratio between actual and potential transpiration) for both the "Static" and

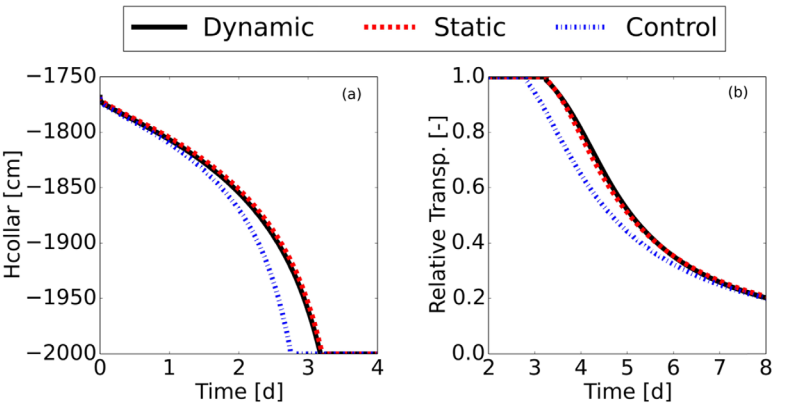

Figure 3. Water head at the (a) root collar and (b) relative transpiration (ratio between the actual and potential transpiration) as a function of time for the different scenarios. Note that stress onset is defined as the time where the collar water potential is equal to -2×10^3 cm.

"Dynamic" scenarios are similar. For those scenarios, the decrease in transpiration starts later (compared to the "Control" scenario) and the curves of the different scenarios meet after day 7 (see Figure 3b).

In Figure 4, the sink profiles for the different scenarios at three different times (1, 4.5, and 9.5 days from the beginning of the simulation) are shown. Initially (i.e., at day 1), a similar homogenous profile of the sink term is observed for all the scenarios. With time, each of the scenarios develops a different profile but for all the scenarios, the uptake is smaller at the upper part of the profile and larger at the bottom of the root. This is due to the vertical fluxes in the profile and the fact that only the apical root nodes received water from three directions. Another interesting observation is that the sink profiles for the "Dynamic" scenario are more uniform than for the "Static" and the "Control" scenarios. This is as the vertical fluxes for the "Dynamic" scenario are also controlled by the nonequilibrium process (see equation (5)) and therefore impeded. The outcome is a more homogeneous water content distribution around the roots (see, for example, Figure 1, where the rhizosphere water content distributions at day 5 for the "Dynamic" and "Static" scenarios are shown), and therefore more homogeneous hydraulic conductivity, which further results in a more homogeneous sink profile (i.e., a positive feedback process).

4.2. Wetting Soil

In Figure 5, a vertical cross section (y = 0) of the water content distribution at different times (starting at t=10.05 day, where the results for t=10 day are show in Figure 1) and for the different scenarios are shown.

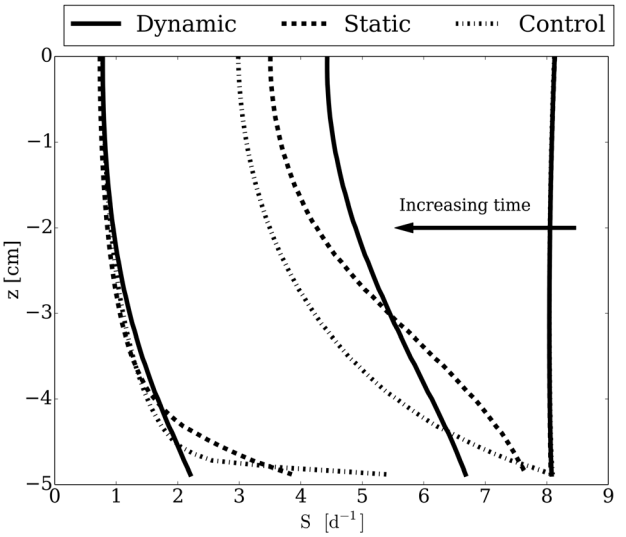

Figure 4. Sink profiles for the different scenarios at different times (1, 4.5, and 9.5 days from the beginning of the simulation).

Recall that the dry soil was wetted with a flux of 55.55 cm/d for 14.4 min (between 10 and 10.01 day). At t=10.05 day, the water content above the wetting front for the "Control" scenario is relatively homogeneous. With time, the wetting front advanced forward. Due to transpiration, the water content in the rhizosphere decreases more rapidly than in the bulk soil (see the lowest right most plot in Figure 5). In contrast, for the "Static" scenario, where the hydraulic properties of the rhizosphere are different from the bulk soil properties (see Figures 3a and 3b), the water content in the rhizosphere is much higher than in the bulk soil (recall that for the "Static" scenario the rhizosphere water holding capacity is higher than the bulk soil).

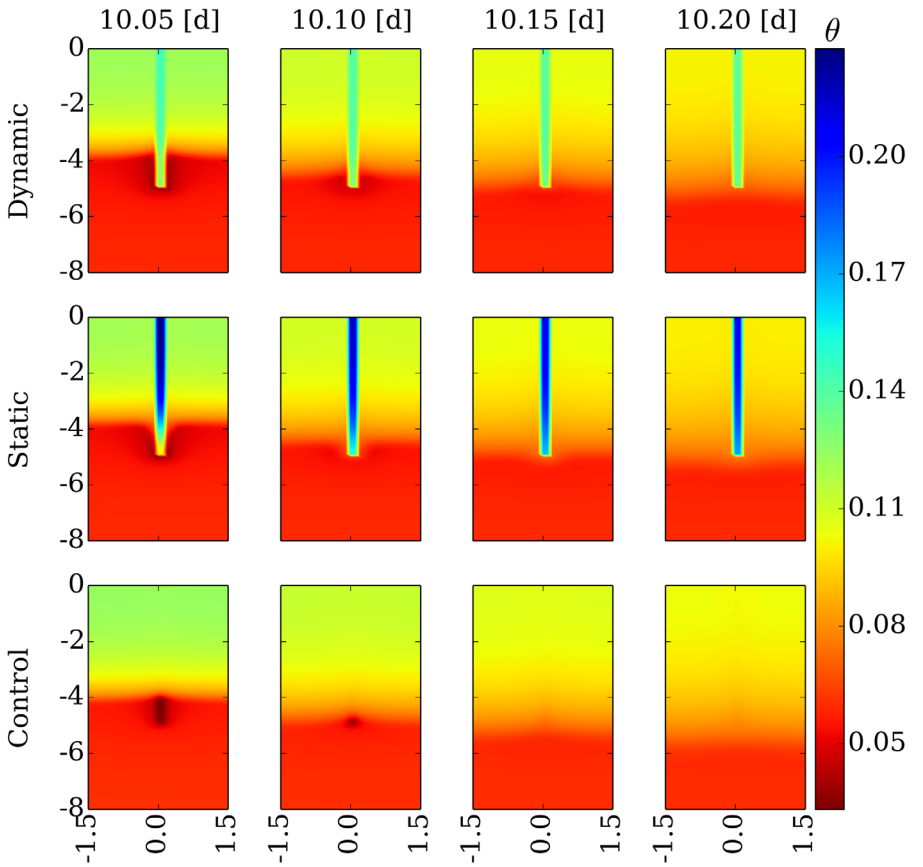

Figure 5. A vertical cross section (y = 0) of the water content distribution for different scenarios at different times after imposing an inward water flux from the top. Note that that the *x* and *z* axis represent the width and depth (in cm) of the domain, respectively (for more clarity not shown in the figure). For better visibility of the root-soil interface, the horizontal and vertical scales are not equal.

For the "Dynamic" scenario, the water content in the rhizosphere is higher than in the bulk soil but the rate of change of the rhizosphere water content is lower than that of the bulk soil. For example, the rate of change in the average water content $(\Delta\theta/\Delta t)$ at the bulk soil and at the rhizosphere between day 10 and day 10.05 is 0.59 and 0.33 day^{-1}, respectively. Note that for both the "Static" and "Control" scenarios, the rate of change in the average rhizosphere water content is higher than for the bulk soil (3 and 4 times higher, respectively). The slower rewetting of the rhizosphere demonstrated here is in a qualitative agreement with the experimental results reported by *Carminati et al.* [2010] and *Moradi et al.* [2012].

In Figure 6, the water content distribution for the rewetting of dry soil $\left(h(t{=}0){=}-1{\times}10^4\ \text{cm}\right)$ is shown. Of most interest is the smaller water content at the rhizosphere of the "Dynamic" scenario (at days 0.12 and 0.14) compared to the bulk soil of this scenario and to the rhizosphere water content of the "Static" and "Control" scenarios. As discussed above, the slower rewetting of the rhizosphere for the "Dynamic" scenario is a result of the nonequilibrium between the water content and matric head (see equation (3)). Furthermore, the relaxation term in equation (3) is inversely related to the water content (equation (9)) and therefore, the drier the rhizosphere, the longer it will take to rewet.

4.3. Drying and Wetting Cycles

To illustrate the impact of nonequilibrium kinetics on the rhizosphere water content during a drying/wetting cycles, the matric head as a function of water content for the "Static" and "Dynamic" scenarios and for the two initial condition (initially wet, IW and initially dry, ID) is shown in Figure 7a (at one point in the rhizosphere, i.e., at x = y = 0; z = −2 cm). Regardless of the initial condition, the "Static" curves are just a reflection of the rhizosphere retention curve (i.e., the hydrostatic retention curve is identical to the hydrodynamic curve). This is also the case for the "Control" scenario (not shown). In contrast, for the "Dynamic" scenario, each wetting/drying cycle is associated with a different matric head—water content relation. Furthermore,

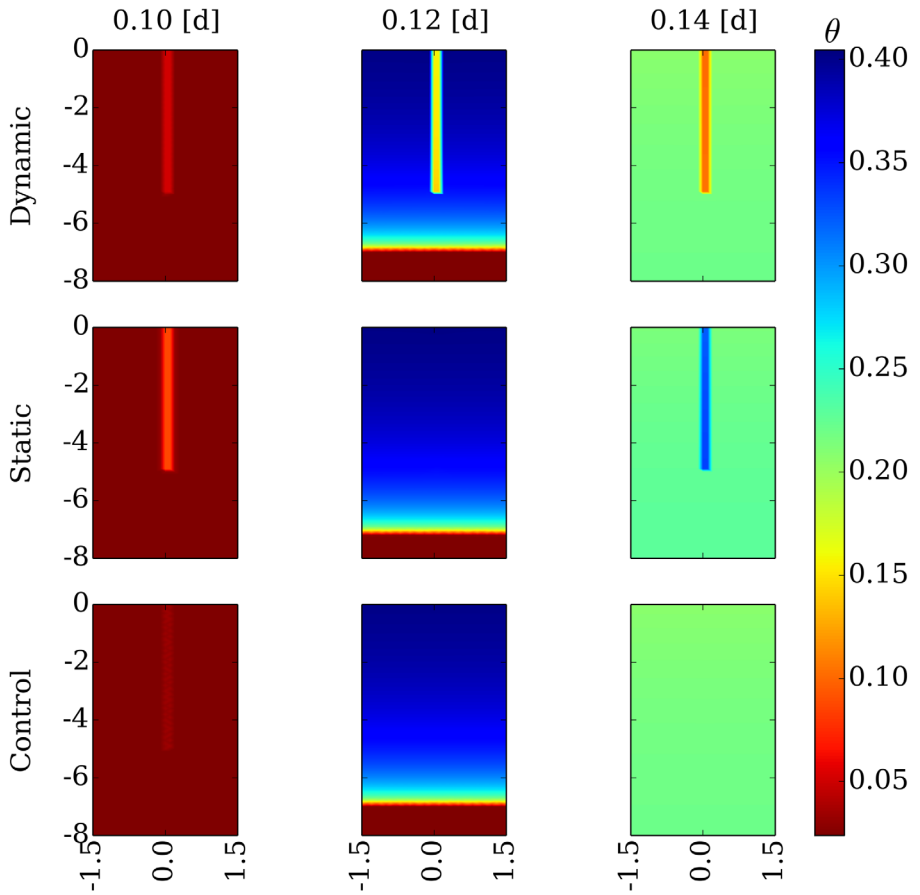

Figure 6. Water content distribution for initially dry soil $(h(t{=}0){=}-1{\times}10^{-4}\,\mathrm{cm})$. Between day 0.1 and 0.12, an inward flux of 730 cm/d is imposed from the upper boundary of the domain. A free drainage boundary condition is imposed at the lower boundary. All other properties are identical to the wetting setup. Note that for better visibility of the root-soil interface, the horizontal and vertical scales are not equal.

the initial condition has a strong effect on the $h(\theta)$ relationship of the "Dynamic" scenario, but with time, the impact of initial conditions weakens and the difference between the "Dynamic_IW" and the "Dynamic_ID" curves becomes smaller (see also Figure 7b).

An outcome of the nonequilibrium relationship between water content and water matric head for the "Dynamic" scenario is the relatively narrow range of water content values in the rhizosphere experienced during the whole simulation. For example, the water content range for the "Dynamic_IW" and the "Dynamic_ID" are $0.11 \leq \theta \leq 0.16$ and $0.05 \leq \theta \leq 0.13$, respectively. For the "Static" scenario, the water content range is $0.09 \leq \theta \leq 0.29$ (see Figure 7b).

In Figure 8, the evolution of transpiration for the different scenarios is shown. The first observation to be made is that stress onset is first occurring for the "Control" scenario and that the total amount of water transpired in this scenario is the lowest (note that this is true regardless of the initial condition; see Figures 8a and 8b). Starting with initially wet soil (Figures 8a, 8c, and 8d), stress onset and the actual transpiration of the "Static" and "Dynamic" scenarios are similar. For example, following the second irrigation cycle (starting at day 15) of the initially wet soil, stress onset after an irrigation event for the "Static" and "Dynamic" scenarios are 7.07 and 6.9 days, respectively (note that for the "Control" scenario stress onset is 6.62 days after irrigation event; see Figure 8a). For both the "Control" and "Static" scenarios, stress onset is not affected by the initial condition. For initially dry soil, stress onset of the "Dynamic" scenario change between irrigation cycles. This is further illustrated in Figure 9 where the difference in stress onsets between the "Dynamic_IW" and the "Dynamic_ID" is shown. It is interesting to note that with every irrigation cycle, stress onset of the "Dynamic_ID" scenario occurs later (recall that for the "Dynamic_IW" scenario, stress onset does not change between the second and the last cycle). That is as for the

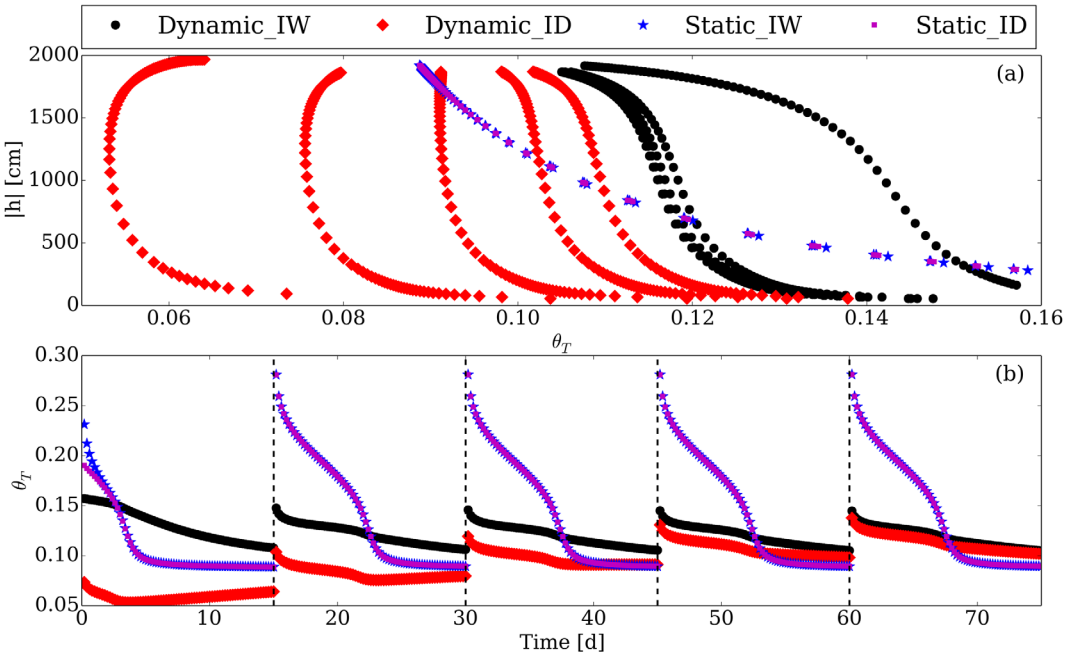

Figure 7. (a) Matric head absolute value as a function of water content and (b) water content as a function of time for the "Dynamic" and "Static" scenarios. For each scenario, both initially wet and initially dry (IW and ID, respectively) conditions are shown. The data shown here are obtained from a point close to the root (x = y = 0; z = −2 cm). Note that for better visibility in Figure 7a we do not show the full range of the "Static" scenario water content (0.09–0.29). Also note that for Figure 7b, the first data are from time 0.2 day.

"Dynamic_ID" scenario, the average water content in the rhizosphere increases between irrigation cycles (see, for example, Figure 7b) which in turn increases the rhizosphere hydraulic conductivity and therefore decreases the hydraulic gradient required to sustain transpiration demand.

5. Discussion

In this study, we investigated the impact of mucilage on soil water dynamics and on RWU by means of numerical simulations with a novel 3-D soil-root model including rhizosphere processes. When we consider a drying soil, the water content distribution for both the "Static" and "Dynamic" scenarios (Figure 1) is in qualitative agreement with high-resolution neutron radiography images of soil showing that the water content in the rhizosphere is higher than in the bulk soil [e.g., *Carminati et al.*, 2010; *Moradi et al.*, 2011]. Wetter rhizosphere results in a higher rhizosphere hydraulic conductivity (see Figures 2b and 2c). As a result, the gradient required to sustain transpiration demand is higher for the "Control" scenario (Figure 3a) and stress onset for the "Static" and "Dynamic" scenarios occurs later (Figure 3b). While this can help plants to transpire under dry condition, a wetter rhizosphere (and therefore dryer bulk soil, see section 4.1) also means that the water reservoirs in the soil are exhausted more rapidly.

As it can be seen from Figures 5 and 6, for the "Dynamic" scenario, rhizosphere rewetting is a slow process (compared to the rewetting of the bulk soil or the rewetting of the rhizosphere of the "Static" or "Control" scenarios), which depends on the relaxation time and on the rhizosphere water content prior to the rewetting. Furthermore, due to the inverse relation between the relaxation time and the water content, drier the rhizosphere the longer it takes to rewet it (see, for example, Figure 7b). During the time that the rhizosphere rewets, roots have a limited access to water, stress onset appears early (see Figures 8b and 8e), and roots cannot support the transpiration demand. The time to rewet the rhizosphere depends on mucilage properties (e.g., degree of hydrophobicity which is accounted for in the relaxation time) and the boundary conditions. In the system examined here, even after five irrigation cycles (with water volume of more than 2 times the pore volume at each irrigation), stress onset for an initially dry rhizosphere appears earlier (see Figure 9).

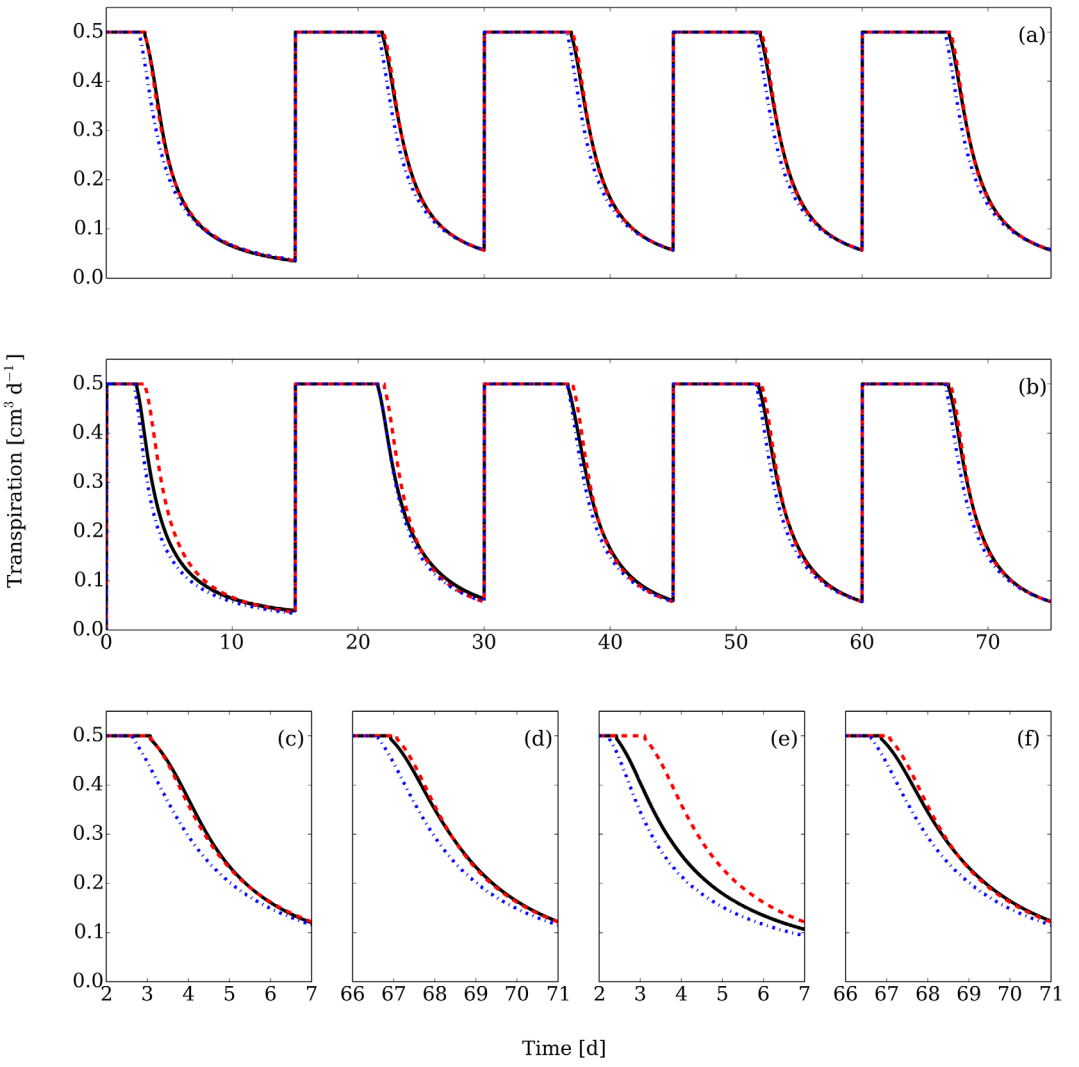

Figure 8. Transpiration as a function of time for the different scenarios ("Dynamic" solid line, "Static" dash line, and "Control" dash dot) and for the (a) wet and (b) dry initial conditions. Enlargement of the (c) first and (d) last stress period of Figure 8a. Enlargement of the (e) first and (f) last stress period of Figure 8b.

The results from the drying and wetting setups show that nonequilibrium ("Dynamic" scenario) delays the impact of boundary condition on rhizosphere water content (and therefore also on RWU). In the case when rhizosphere is wetter than the bulk soil, this delay allows the plant to better support transpiration demand. On the other hand, the "temporal isolation" of the root from the bulk soil means that the plant response to stress (e.g., by closing the stomata) will be activated in a delay. If the rhizosphere is drier than the bulk soil, the plant might experience water stress despite the availability of water at the bulk soil (see, for example, upper right plot in Figure 6). In this case, leaching of water and nutrient below the root zone is higher.

It is interesting to note that despite large variations in matric head, the fluctuation of the rhizosphere water content for the "Dynamic_IW" or the "Dynamic_ID" remains relatively small (in contrast to the "Static" or "Control" scenarios, see Figure 7a). Other natural polymers such as extracellular polymeric substances (EPS) were also found to decrease fluctuation in hydration condition of porous media [e.g., *Or et al*., 2007a, 2007b] . Since the rhizosphere is one of the richest microbial zones in the soil and as microbes play an essential role in plant nutrition and growth promotion [*Marschner et al*., 2001], it is possible that another biological function of mucilage is to protect rhizosphere bacteria from rapid changes in their vicinity [see also *Or et al*., 2007b].

Comparing the "Static" and "Dynamic" scenarios shows that in order to capture water content distribution in the rhizosphere during a wetting process (i.e., slower rewetting of the rhizosphere and rhizosphere that

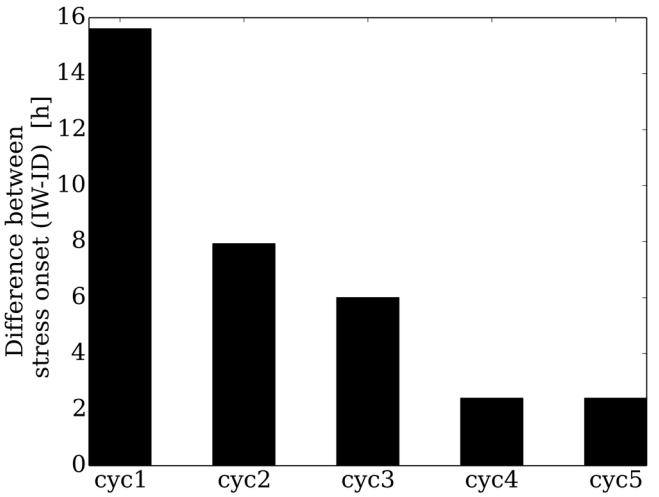

Figure 9. Difference between stress onsets of the initially wet (IW) and initially dry (ID) "Dynamic" scenarios for each irrigation cycle. Note that except in cyc1 stress onset of the "Dynamic_IW" scenario did not change between irrigation cycles.

is drier than bulk soil), nonequilibrium has to be included in the flow model (Figures 5 and 6). On the other hand, for a drying process, the rhizosphere of both the "Static" and "Dynamic" scenarios is wetter than the bulk soil (e.g., Figure 1). Indeed, for wetting processes, there are two main theoretical explanations for the development of nonequilibrium in the rhizosphere. First, the jelly-like properties of mucilage imply that the rewetting of dry mucilage is a kinetic process governed by the diffusion rate of polymer network into water [*Tanaka et al*., 1985]. Second, mucilage contains amphiphilic substances (e.g., surfactants) which might show hydrophobic properties when rewetted [*Carminati and Vetterlein*, 2013]. Those two mechanisms can be formulated as a nonequilibrium process as they will slow down the increase in water content of dry rhizosphere. Based on the above, we argue that for a wetting process there are both theoretical and experimental evidences that justified the introduction of nonequilibrium dynamics in rhizosphere flow models. For a drying process, it is not clear to which extent nonequilibrium is needed to be included in the flow model and a further research is needed in order to clarify this issue.

6. Conclusion

We have presented a novel detailed 3-D soil-root water flow model that accounts for rhizosphere-specific processes. Our numerical simulations show that nonequilibrium (due to mucilage exudate) slows down rhizosphere drying and rewetting. As a result, the temporal variations of water content in the rhizosphere strongly depend on the rhizosphere water content prior to the changes in boundary conditions. That means, for example, that an irrigation event at wet or dry conditions leads to different behavior such as earlier and longer stress for drier rhizosphere. Furthermore, rhizosphere is characterized by a more homogeneous profiles of water content and hydraulic conductivity and therefore (in a positively feedback process) also of the sink term. Finally, fluctuations in water content in the rhizosphere are lower than in the bulk soil, so the root surface is less exposed to rapid environmental changes.

Overall, the model provides a tool to further examine the impact of different processes at the rhizosphere scale on water dynamics and RWU. Some issues that require further investigation are:

1. In this work, we assume that mucilage is evenly distributed along the root. Yet there are evidences suggesting that mucilage concentration and properties change with time [*Carminati*, 2013]. While in the current model, it is simple to consider the spatiotemporal distribution of mucilage an experimental data and theoretical understanding of mucilage distribution (and probably also mucilage degradation) is still missing.
2. In the present work, we only considered a single root. That means, for example, that only a qualitative analysis of the relative contribution of mucilage to RWU was feasible. Analysis of the impact of the root hydraulic architecture and rhizosphere distribution will be carried out in a further study.
3. The mechanisms causing nonequilibrium in the rhizosphere need to be better understood. Specifically, it needs to be determined to which extent nonequilibrium between water content and water potential needs to be considered during a drying process.
4. The impact of root growth on the architecture of the rhizosphere (e.g., bulk density and pore size distribution) and root water uptake need to be studied.

Acknowledgments
The complete data set is available on demand to N. Schwartz. N.S. is supported through a postdoctoral grant from the "Fond Spécial de la Recherche" of the Université catholique de Louvain (FSR), cofunded by the European Commission through the COFUND program. We thank Teamrat Ghezzehei and two additional anonymous reviewers for their constructive comments that significantly improved the quality of this paper.

References

Ahmed, M. A., E. Kroener, M. Holz, M. Zarebanadkouki, and A. Carminati (2014), Mucilage exudation facilitates root water uptake in dry soils, *Funct. Plant Biol.*, *41*(11), 1129–1137, doi:10.1071/FP13330.

Aravena, J. E., M. Berli, S. Ruiz, F. Suárez, T. A. Ghezzehei, and S. W. Tyler (2013), Quantifying coupled deformation and water flow in the rhizosphere using X-ray microtomography and numerical simulations, *Plant Soil*, *376*, 95–110, doi:10.1007/s11104-013-1946-z.

Brooks, R. H., and A. T. Corey (1964), Hydraulic Properties of Porous Media, *Hydrol. Pap. 3*, Colo. State Univ., Fort Collins.

Carminati, A. (2012), A model of root water uptake coupled with rhizosphere dynamics, *Vadose Zone J.*, *11*(3), doi:10.2136/vzj2011.0106.

Carminati, A. (2013), Rhizosphere wettability decreases with root age: A problem or a strategy to increase water uptake of young roots?, *Front. Plant Sci.*, *4*, 298, doi:10.3389/fpls.2013.00298.

Carminati, A., and D. Vetterlein (2013), Plasticity of rhizosphere hydraulic properties as a key for efficient utilization of scarce resources, *Ann. Bot.*, *112*(2), 277–290, doi:10.1093/aob/mcs262.

Carminati, A., A. B. Moradi, D. Vetterlein, P. Vontobel, E. Lehmann, U. Weller, H.-J. Vogel, and S. E. Oswald (2010), Dynamics of soil water content in the rhizosphere, *Plant Soil*, *332*(1-2), 163–176, doi:10.1007/s11104-010-0283-8.

Daly, K. R., S. J. Mooney, M. J. Bennett, N. M. J. Crout, T. Roose, and S. R. Tracy (2015), Assessing the influence of the rhizosphere on soil hydraulic properties using X-ray computed tomography and numerical modelling, *J. Exp. Bot.*, *66*(8), 2305–2314, doi:10.1093/jxb/eru509.

de Jong van Lier, Q., K. Metselaar, and J. C. van Dam (2007), Root water extraction and limiting soil hydraulic conditions estimated by numerical simulation, *Vadose Zone J.*, *6*(3), 527, doi:10.2136/vzj2007.0042L.

Doussan, C. (1998), Modelling of the hydraulic architecture of root systems: An integrated approach to water absorption—Model description, *Ann. Bot.*, *81*(2), 213–223, doi:10.1006/anbo.1997.0540.

Doussan, C., A. Pierret, E. Garrigues, and L. Pagès (2006), Water uptake by plant roots: II—Modelling of water transfer in the soil root-system with explicit account of flow within the root system—Comparison with experiments, *Plant Soil*, *283*(1-2), 99–117, doi:10.1007/s11104-004-7904-z.

Gardner, W. R. (1960), Dynamic aspects of water availability to plants, *Soil Sci.*, *89*(2), 63–73.

Garrigues, E., C. Doussan, and A. Pierret (2006), Water uptake by plant roots: I—Formation and propagation of a water extraction front in mature root systems as evidenced by 2D light transmission imaging, *Plant Soil*, *283*(1-2), 83–98, doi:10.1007/s11104-004-7903-0.

Ghezzehei, T. A., and A. A. Albalasmeh (2015), Spatial distribution of rhizodeposits provides built-in water potential gradient in the rhizosphere, *Ecological Modell.*, *298*, 53–63, doi:10.1016/j.ecolmodel.2014.10.028.

Hartmann, A., M. Rothballer, and M. Schmid (2007), Lorenz Hiltner, a pioneer in rhizosphere microbial ecology and soil bacteriology research, *Plant Soil*, *312*(1-2), 7–14, doi:10.1007/s11104-007-9514-z.

Hassanizadeh, S. M., M. A. Celia, and H. K. Dahle (2002), Dynamic effect in the capillary pressure–saturation relationship and its impacts on unsaturated flow, *Vadose Zone J.*, *1*(1), 38–57, doi:10.2136/vzj2002.3800.

Jasechko, S., Z. D. Sharp, J. J. Gibson, S. J. Birks, Y. Yi, and P. J. Fawcett (2013), Terrestrial water fluxes dominated by transpiration, *Nature*, *496*(7445), 347–350, doi:10.1038/nature11983.

Javaux, M., T. Schröder, J. Vanderborght, and H. Vereecken (2008), Use of a three-dimensional detailed modeling approach for predicting root water uptake, *Vadose Zone J.*, *7*(3), 1079–1088, doi:10.2136/vzj2007.0115.

Kroener, E., M. Zarebanadkouki, A. Kaestner, and A. Carminati (2014), Nonequilibrium water dynamics in the rhizosphere : How mucilage affects water flow in soils, *Water Resour. Res.*, *50*, 6479–6495, doi:10.1002/2013WR014756.

Landsberg, J. J., and N. D. Fowkes (1978), Water movement through plant roots, *Ann. Bot.*, *42*, 493–508.

Marschner, P., C.-H. Yang, R. Lieberei, and D. E. Crowley (2001), Soil and plant specific effects on bacterial community composition in the rhizosphere, *Soil Biol. Biochem.*, *33*(11), 1437–1445, doi:10.1016/S0038-0717(01)00052-9.

McCully, M. E., and J. S. Boyer (1997), The expansion of maize root-cap mucilage during hydration. 3. Changes in water potential and water content, *Physiologia Plantarum*, *99*, 169–177.

Moradi, A. B., A. Carminati, D. Vetterlein, P. Vontobel, E. Lehmann, U. Weller, J. W. Hopmans, H.-J. Vogel, and S. E. Oswald (2011), Three-dimensional visualization and quantification of water content in the rhizosphere, *New Phytol.*, *192*(3), 653–663, doi:10.1111/j.1469-8137.2011.03826.x.

Moradi, A. B., A. Carminati, A. Lamparter, S. K. Woche, J. Bachmann, D. Vetterlein, H.-J. Vogel, and S. E. Oswald (2012), Is the rhizosphere temporarily water repellent?, *Vadose Zone J.*, *11*(3), doi:10.2136/vzj2011.0120.

Mualem, Y. (1976), A new model for predicting the hydraulic conductivity of unsaturated porous media, *Water Resour. Res.*, *12*(3), 513–522.

Or, D., S. Phutane, and A. Dechesne (2007a), Extracellular polymeric substances affecting pore-scale hydrologic conditions for bacterial activity in unsaturated soils, *Vadose Zone J.*, *6*(2), 298–305, doi:10.2136/vzj2006.0080.

Or, D., B. F. Smets, J. M. Wraith, A. Dechesne, and S. P. Friedman (2007b), Physical constraints affecting bacterial habitats and activity in unsaturated porous media—A review, *Adv. Water Resour.*, *30*(6-7), 1505–1527, doi:10.1016/j.advwatres.2006.05.025.

Read, D. B., and P. J. Gregory (1997), Surface tension and viscosity of axenic maize and lupin root mucilages, *New Phytologist*, *137*, 623–628, doi:10.1046/j.1469-8137.1997.00859.x.

Richards, L. A. (1931), Capillary conduction of liquids through porous mediums, *Physics*, *1*, 318–333.

Roose, T., and A. C. Fowler (2004), A mathematical model for water and nutrient uptake by plant root systems, *J. Theor. Biol.*, *228*(2), 173–184, doi:10.1016/j.jtbi.2003.12.013.

Rovira, A. D. (1956), Plant root excretions in relation to the rhizosphere effect, *Plant Soil*, *7*(2), 178–194, doi:10.1007/BF01343726.

Schneider, C. L., S. Attinger, J.-O. Delfs, and A. Hildebrandt (2009), Implementing small scale processes at the soil-plant interface—The role of root architectures for calculating root water uptake profiles, *Hydrol. Earth Syst. Sci. Discuss.*, *6*(3), 4233–4264, doi:10.5194/hessd-6-4233-2009.

Schroeder, T., M. Javaux, J. Vanderborght, B. Koerfgen, and H. Vereecken (2008), Effect of local soil hydraulic conductivity drop using a three-dimensional root water uptake model, *Vadose Zone J.*, *7*, 1089–1098, doi:10.2136/vzj2007.0114.

Tanaka, T., E. Sato, Y. Hirokawa, S. Hirotsu, and J. Peetermans (1985), Critical kinetics of volume phase transition of gels, *Phys. Rev. Lett.*, *55*(22), 2455–2458, doi:10.1103/PhysRevLett.55.2455.

Tuzet, A., A. Perrier, and R. Leuning (2003), A coupled model of stomatal conductance, photosynthesis and transpiration, *Plant Cell Environ.*, *26*(7), 1097–1116, doi:10.1046/j.1365-3040.2003.01035.x.

Zarebanadkouki, M., and A. Carminati (2014), Reduced root water uptake after drying and rewetting, *J. Plant Nutr. Soil Sci.*, *177*(2), 227–236, doi:10.1002/jpln.201300249.